Fall 2016

The Effect of Protein Import on Membrane Potential

Ruth Hartke
CUNY Bernard M Baruch College

Honors Thesis:

The Effect of Protein Import on Membrane Potential

Ruth E. Hartke

Submitted to the committee of Undergraduate Honors at Baruch College of the City University of New York on December 5, 2016 in partial fulfillment of the requirements for the degree of Bachelor of Arts in Biology with Honors.

I dedicate this thesis to my father, who fostered my curiosity and ambition and wholeheartedly supported my every dream.

Acknowledgements

Dr. Pablo Peixoto
Dr. Jean Gaffney
Dr. Helene Eisenman Barbour
Dr. Krista Dobi
The Mitochondriacs

Table of Contents

Abstract

Mitochondria are essential organelles often referred to as the “power plants” of eukaryotic cells. Energy conversion in mitochondria relies on oxidation of metabolite intermediates by protein components of the electron transport chain and establishment of an electrochemical gradient across the inner membrane. Some of the proteins involved are encoded by mitochondrial DNA, but the vast majority, over 98%, has to be imported from the cytosol. Protein import complexes form pores in the outer and inner membranes to mediate the process. However, opening of these pores would in theory jeopardize formation of the electrochemical gradient. In this study we examined this possibility by measuring membrane potential of yeast mitochondria during protein import using spectrofluorimetry and fluorescence microscopy. Contrary to expectation, our results suggest that treatment with import peptides hyperpolarize mitochondria, provided that the import pores are expressed. If confirmed in other experimental models, these results may help determine a potential preventive mechanism that allows the co-existence of protein import and an electrochemical gradient across the inner membrane.

1. Introduction

In the eukaryotic world, mitochondria are known as the powerhouses of the cell for their ability to produce ATP, the energy currency of biological reactions. In order to perform the vital functions of cellular respiration and energy production, a large cast of proteins and smaller molecules such as nucleotides and metabolites are incorporated into the workings of this organelle. In accordance with the endosymbiont theory, mitochondria contain a separate genome (mtDNA) from nuclear DNA and contain the machinery allowing mitochondria to be capable of transcribing and translating proteins[1]. However, over time, mitochondria have lost the ability to produce all but 13 proteins, while the other 1145 [2] proteins are nuclear encoded, translated by cytosolic ribosomes, and imported into the mitochondria [3, 4]. The import of proteins is necessary for mitochondria to complete physiologically crucial processes. One such process, completed by the oxidative phosphorylation system, provides organisms with ATP [5].

At the core of energy production are a set of 5 protein complexes located on the inner membrane of mitochondria, known as the electron transport chain (ETC). Through a series of oxidation-reduction reactions, hydrogen atoms are stripped from Kreb's cycle intermediates by the first two respiratory protein complexes of the ETC of the mitochondrial inner membrane. Further oxidation of electrons through the ETC is accompanied by proton pumping into the intermembrane space. The collection of positive charges outside in the intermembrane space creates a potential difference across the inner membrane known as the membrane potential [5]. ATP is produced with Complex V, or ATP Synthase. ATP synthase is a part of the electron transport chain and utilizes membrane potential in the same way a dam uses the flow of water to create energy used to propel an energy-converting turbine. Protons are allowed to flow down the gradient from high concentration in the intermembrane space to low concentration in the matrix. This flow of

electrons through what is known as the F_0 portion of Complex V incites the spinning of F_0 and F_1 subcomplexes. This spinning action of F_1 catalyzes the formation of ATP from ADP and P_i [6].

A number of nuclear encoded proteins are necessary to contribute to the process of energy production, and therefore must be imported into mitochondria. For example, Coenzyme Q synthase, an enzymatic protein complex responsible for assembling ubiquinone of Complex II within the matrix of mitochondria, must first import its nuclear encoded subunits [7]. Additionally, all but one subunit of the cytochrome bc_1 complex or Complex III is imported from the cytosol [8]. The pathways of import utilize highly conserved protein complexes within the outer and inner membranes of mitochondria of yeast [9] (Figure 1). Most import pathways stem from Translocase of the Outer Membrane (TOM). From TOM, a protein can be inserted into the outer membrane through (SAM), remain in the intermembrane space with the aid of MIA, be inserted into the inner membrane by way of TIM22 or TIM23, or enter the matrix through TIM23. Inner membrane proteins chaperoned by the small protein complex Tim9-Tim10 are brought to TIM22 for lateral release. Conversely, inner membrane bound proteins containing a matrix targeted presequence import via TIM23. Proteins containing a positively charged amino terminal presequence are imported to the matrix where the presequence is cleaved by proteolysis. Other proteins with stop transfer residues are stalled in the channel, presequence residues in the matrix are cleaved, and the protein is transferred laterally into the inner membrane [10]. The half-life of mitochondrial proteins can range from 30 hours to several days; however, mitochondria possess an extensive proteolytic enzyme system necessary not only for cleaving presequences, but also for quality control. Additionally, the action of this system also prevents protein and peptide overload, which would otherwise lead to apoptosis [11, 12]. The result is that there is a high protein turnover rate necessitating the constant renewal of internal machinery.

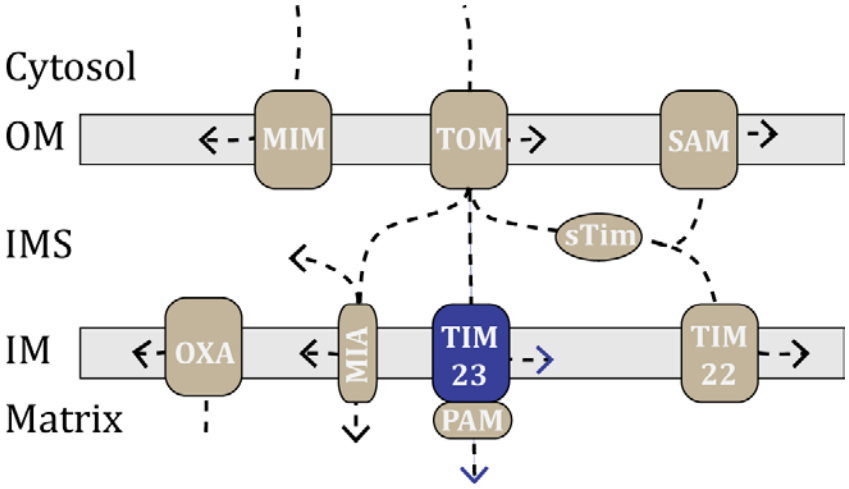

Figure 1: Import pathways into mitochondria. Proteins with a matrix targeting sequence import through the outer membrane (OM) via the TOM complex and through the inner membrane (IM) via TIM23. Modified from Aung et. al., 2017 [13].

Not only does the ETC rely on the import of proteins to facilitate its proton pumping and energy producing abilities, but import of proteins also relies on the energy gradient produced by ETC machinery. An example of this symbiotic relationship is the import of the enzyme glutamate dehydrogenase, a vital enzyme that converts glutamate to α-ketoglutarate in the matrix[14]. Glutamate dehydrogenase is nuclear encoded and must be imported into mitochondria in order to function. The mature protein contains a relatively long cleavable presequence with two arginine resides and a lysine residue containing positive charges. The positively charged residues utilize the membrane potential gradient that draws it through the TIM23 complex [15]. An additional layer to the codependent nature of the relationship is the need for ATP in the cytosol in order for membrane bound proteins to reach the mitochondria before mitochondrial machinery takes over import [10, 16].

One question motivating this thesis research is how the action of importing proteins affects membrane potential in the process. The TIM23 complex contains two subunits, Tim23 and Tim17 responsible for forming the double barrel pore through which proteins enter the matrix. It has been experimentally estimated that the size of these pores in their open state range from 0.81-0.94 nm [17], which is 6 orders of magnitude larger than the proton pore of respiratory Complex V [18].

2. Objective

This study aims at determining the effects of protein import on mitochondrial membrane potential.

3. Materials and Methods

3.1. Growth and maintenance of yeast model

1. Baker's yeast *Saccharomyces cerevisiae* Tim23 conditional knockdown (Tim23 Gal10) genotype #6423819.
2. Sterile Erlenmeyer flasks capped with a cotton plug
3. Inoculating loops
4. SDLac -Leu +Gal, 1X : 2% Dextrose (J.T. Baker, cat. #1916-05), 0.5% Galactose (Fisher, cat. #BP656-500), Adenine hemisulfate 27.2 mg/L (Sigma-Aldrich, cat. #A9126), Uracil 20 mg/L (Sigma, cat. #U0750), L-Tryptophan 33.4 mg/L (Sigma-rich, cat. #T0254), L-Histidine 33.4 mg/L (Sigma, cat. #H-8125), L-Lysine 41.6 mg/L (Sigma-Aldrich, cat. #L5626), Yeast Nitrogen Base w/o amino acids 1.7 g/L (Sigma-Aldrich, cat. #Y0626), Ammonium Sulfate 5 g/L (Fisher, cat. #A702500), 2% Sodium Lactate (Fisher, cat. #S326 500)
5. SDLac – Leu – Gal, 1X: contains the same reagents as SDLac minus galactose
6. SDLac – Leu +Gal, 2% agar poured in sterile petri dishes
7. New Brunswick Scientific – Excella E24 Incubator Shaker Series
8. Thermo Scientific Genesys20 Spectrophotometer

3.2. Generating Growth Curves

Yeast were initially thawed from frozen stocks and inoculated onto SDLac +Gal medium and 2% agar plates at 32° C for approximately 72 hours. Single colonies were inoculated into 20 mL liquid SDLac +Gal medium in a 125 mL sterile Erlenmeyer flask and incubated in a shaker at 32° C, 250 rpm for approximately 48-72 hours. Conditional knocking down of Tim23 was achieved by growing cultures in SDLac medium in absence of galactose (-Gal) [19]. A linear growth curve of in the presence or absence of galactose was generated by measuring optic densities at 600 nm (OD) once every 2 hours. An initial OD of 0.1 was considered time 0, with subsequent measurements generated for the following 22 to 26 hours until the stationary growth phase was reached.

In order to produce qualitative growth curves, plates were poured with SDLac +Gal, 2% agar and SDLac –Gal, 2% agar respectively. Yeast grown in SDLac +Gal medium to an OD of 1, was serially diluted 4 orders of magnitude and spread onto each plate in 10 μL volumes. Plates were incubated at 32° C for 42 hrs.

3.3. Measuring Membrane Potential in Intact Yeast

1. Baker's yeast *Saccharomyces cerevisiae* Tim23 conditional knockdown (Tim23 Gal10).
2. New Brunswick Scientific – Excella E24 Incubator Shaker Series
3. Thermo Scientific Genesys20 Spectrophotometer
4. 1.5 mL microcentrifuge tubes
5. Sorvall Legend Micro 17 microcentrifuge
6. FTS-Systems, Vacuum pump
7. Molecular Devices – Spectra Max M2 Plate Reader
8. 1X Phosphate-buffer solution (PBS) (Fisher, cat. #BP13061)

9. Tetramethylrhodamine, methyl ester (TMRM) (Sigma-Aldrich, cat. #T5428)
10. Nikon TE2000 Eclipse Inverted Fluorescence Microscope Equipped with CCD camera of 8 MP, automated shutters and filter cubes, Xenon fluorescence bulb
11. NIS Elements v. 4.3 by Nikon

Starting at an OD of 0.1, Tim23 Gal10 yeast were grown in SDLac medium in the presence or absence of galactose overnight at 225 rpm, 30° C. After 12 hours of growth, the OD was measured at 600 nm. Yeast were diluted with SDLac to an OD of 0.5, an optimal cellular density for TMRM labeling, and prepared in 1 mL volumes. TMRM was added to 1 mL samples of yeast for a final concentration of 1 μM. Samples were incubated in the dark at room temperature for 15 minutes. Yeast were placed in the centrifuge and spun at 12,000 rpm for 5 minutes. Using a vacuum pump, the supernatant was removed and samples were resuspended in 1 mL filtered PBS. Two additional PBS washing steps were performed. TMRM was observed by fluorescence microscopy using a Texas Red filter and 40x lenses. Images were recorded using a CoolSnap CCD camera and NIS Elements software.

3.4. Growth for Mitochondrial Isolation

Yeast were grown as described above and to a volume of 200 mL and optic density between 1 and 2. Galactose medium was removed by centrifugation at 4700 rpm for 8 minutes and the pellet was resuspended in water. The procedure was repeated twice prior to resuspending the pellet in 200 mL galactose free medium to an optic density of 0.1 in a 1 L Erlenmeyer flask. The culture was incubated 16 hours prior to isolation at 225 rpm and 32° C.

3.5. Isolation of Mitochondria from Yeast

1. 200 mL cultures of Tim23 Gal10 *S. cerevisiae* at an OD of between 1 and 2 grown in the presence or absence of galactose
2. Sorvall 04146 centrifuge tubes
3. Thermo Scientific centrifuge tube, 28.7 mm
4. Sorvall Dryspin, bo-Oa26, centrifuge bottles
5. Nalgene round 50 mL centrifuge tubes
6. Sorvall 16 mL centrifuge tubes
7. Sorvall Centrifuge RC5C-Plus
8. Sorvall ss-34 centrifuge rotor
9. Sorvall SLA-1500 rotor
10. Mettler Delta Range Analytical Balance
11. Thermo Scientific Genesys20 Spectrophotometer
12. Molecular Devices Spectrophotometer
13. Pre-digestion buffer- 0.1 M Tris(hydroxymethyl)aminomethane (Fisher, cat. #T395-1), pH 9.4 (with H_2SO_4), 10 mM Dithiotreitol (Fisher, cat. #AC42638-0100)
14. Wash buffer- 1.2 M D-Sorbitol (Acros, cat. #132730025), pH 7.4
15. Digestion buffer- 1.2 M Sorbitol, 20 mM Potassium Phosphate (Sigma, cat. #P5655), pH 7.4
16. Lyticase (Sigma, cat. #SLBN1924V)
17. Thermo Scientific Incubator, model 120
18. Homogenization buffer - 0.6 M Sorbitol (Acros, cat. #132730025), 10 mM Tris (Fisher, cat. #T395-1), pH 7.4, 1 mM Ethylenediaminetetraacetic acid (EDTA) (Corning, cat. #MT46034CI), 0.2% Bovine Serum Albumin (BSA)(Fisher, cat. #BP9714), 1 mM Phenylmethane sulfonyl fluoride (PMSF) (Sigma, cat. # A0337900), Protease Inhibitor Cocktail, 5 μL/mL (Sigma, P8215-1ML)

19. Dounce homogenizer (Fisher, S 828)
20. Nikon TE2000 Eclipse Inverted Fluorescence Microscope Equipped with CCD camera of 8 MP, automated shutters and filter cubes, Xenon fluorescence bulb
21. Ice
22. 1 mL microcentrifuge tubes

3.5.1. Digestion of Cell Wall

Just prior to isolation, yeast were observed under the microscope at 40X to check for bacterial contamination and the OD was measured to ensure proper growth. Both cultures were transferred to Sorvall centrifuge bottles and centrifuged 5 minutes at 7000 rpm, 4° C with the SLA-1500 rotor. The supernatant was discarded and the pellet resuspended with deionized water. Each culture was again centrifuged for 5 minutes at 7000 rpm. Pellets were weighed and resuspended at 0.5 g cells / mL in pre-digestion buffer in order to weaken the cell wall. The cells were incubated at 30° C and 100 rpm for 15 minutes. Following incubation, 40 mL of wash buffer was added to remove DTT and restore the pH to neutral. The cells were centrifuged at 7000 rpm for 5 minutes in the ss-34 rotor. The ss-34 rotor was used for each subsequent centrifugation step. This washing step was repeated twice more. Following the third washing step, each pellet was weighed and resuspended in digestion buffer to a concentration of 0.15 g cell/mL. The OD_{800} was recorded as $time_0$ for lyticase treatment. Lyticase was added to cells at a concentration of 2 mg / g of cell. Each sample was placed in a 30° C water bath and mixed with a stir bar during lyticase reaction. The OD_{800} was read after 15 minutes and every subsequent 5 minutes following until the OD_{800} decreased by 80%. The yeast were also observed under microscopy in order to visualize the formation of spheroplasts. Once lyticase treatment was complete, cold wash buffer was added to stop the reaction. The samples were centrifuged at 7000 rpm for 5 minutes.

3.5.2. Homogenization of Yeast

Following the formation of yeast spheroplasts, the pellets were once again weighed and resuspended in homogenization buffer at a concentration of 0.15 g cells / mL. Protease inhibitors were added to the homogenization buffer immediately prior to use. Using a dounce homogenizer and drill set to 120 V, yeast were homogenized by using 10-15 strokes while on ice. The samples were left on ice for 5 minutes. The samples were diluted in one volume with homogenization buffer for a concentration of 0.075 g cells/mL. Using 16 mL centrifuge tubes, the samples were centrifuged in the ss-34 rotor at 3000 rpm for 10 minutes. The supernatant, containing crude isolated mitochondria, was saved and placed on ice. The remaining pellet was once again resuspended in homogenization buffer at the same volume used for dounce homogenization. The dounce homogenizer was utilized a second time for 5 strokes at 120 V. The cells homogenized for the second time were centrifuged at 3000 rpm for 10 minutes. The supernatant was combined with the original supernatant and placed on ice. Yeast were centrifuged at 13,000 rpm for 10 minutes in the ss-34 rotor to produce a crude mitochondrial pellet. The supernatants were discarded and the pellets were gently resuspended in 15-20 mL homogenization buffer. The samples were then centrifuged at 4000 rpm for 10 minutes in order to further purify mitochondrial samples. The supernatants containing isolated mitochondria were collected and transferred to separate centrifuge tubes. The samples were then centrifuged at 13,000 rpm for 10 minutes in order to collect purified mitochondrial pellets. The supernatant was discarded and lipids were wiped from the centrifuge tube walls using Kim-wipes. Using a micropipetter set at approximately 70 μL, the mitochondrial pellet was gently resuspended with the small volume of homogenization buffer left in the bottom of the tube by pipetting the liquid over the pellet taking care not to produce bubbles. The volume of mitochondria in homogenization buffer was measured using the same micropipetter and the samples were stored on ice in 1mL microcentrifuge tubes.

3.6. Quantification of Mitochondrial Proteins

1. 1 mL microcentrifuge tubes
2. 96-well plate
3. Pierce BCA Protein Assay Kit (Thermo Fisher, cat #23227)
4. Spectramax M2 Spectrophotometric plate reader (Perkin Elmer, Inc.)
5. BSA (Fisher, BP9714) standards in the following concentrations (mg BSA / mL deionized water): 2, 1.5, 1, 0.5, 0.25, 0.1, and 0
6. Isolated yeast mitochondria in homogenization buffer
7. Fisher brand Finnpipette II

A 10:1 dilution of each mitochondrial stock was prepared by pipetting 5μL of mitochondria and 45 μL deionized water into a 1 mL microcentrifuge tube. In a 96-well plate, 20 μL of BSA standards were plated in duplicate in increasing concentration. 20 μL of + Gal yeast were pipetted immediately after flicking each microcentrifuge tube and plated in wells side by side. In the same way, 20 μL of – Gal yeast were plated in wells A3 and A4. 200 μL of BCA was added to each well. The plate was mixed by tapping and incubated for 30 minutes at 37° C. Following incubation, the absorbance was measured at 562 nm. A standard curve was then generated using Microsoft Excel and used to determine mitochondrial protein concentration.

3.7. Protein Import Experiment

1. 96 well plate
2. + Gal and –Gal yeast mitochondrial samples
3. Import Buffer: 0.6 M Sorbitol (Acros, cat. # 132730025), 25 mM Potassium Chloride (Fisher, cat. #BP366-1), 10 mM Magnesium Chloride, 2 mM Potassium Phosphate (Sigma, cat.

#P5655), 0.5 mM EDTA (Corning, cat. #MT46034CI), 50 mM Hepes (Fisher, cat. #BP-2937-100) – Potassium hydroxide (Fisher, cat. #P250-1), pH 7.4

4. 0.1 M ATP (Sigma, cat. #A2382) stock prepared in deionized water
5. 0.1 M NADH (Sigma, cat. #N4505) stock prepared in Trizma Buffer: 1.25 M Tris (Fisher, cat. #T395-1), pH 7.0
6. Signal peptide: Cytochrome oxidase subunit IV (yCoxIV) $_{1\text{-}13)}$ ^{1} MLSLRQSIRFFKY$_{13}$
7. Synthetic signal peptide: SynB2 $_{(1\text{-}20)}$ ^{1}MLSRQQSQRQSRQQSQRQSR$_{20}$
8. Carbon cyanide-4-(trifluoromethoxy) phenylhydrazone (FCCP), 40 mM stock (Sigma-Aldrich, C2920)
9. Mitotracker red FM, 0.05 mM stock (Thermo Fisher, cat. #M22425)
10. 200 proof Ethanol (Fisher, cat. #9990520)
11. Thermo Scientific Model 120 Incubator
12. Spectrophotometer
13. Micropipettes and tips
14. 1 mL microcentrifuge tubes
15. Nikon TE2000 Eclipse Inverted Fluorescence Microscope Equipped with CCD camera of 8 MP, automated shutters and filter cubes, Xenon fluorescence bulb
16. NIS Elements v. 4.3 by Nikon

First, 0.1 M ATP and 0.1 M NADH were added to the import buffer at a concentration of 20μL/mL. The BCA protein quantification assay was used to determine the volume of mitochondrial sample needed to add 10μg of mitochondria to each well. Each experimental condition was run in quadruplicate if mitochondrial yield permitted, otherwise in triplicate. The import reactions were assembled in 1 mL microcentrifuge tubes and added to the 96 well plate following the addition of Mitotracker Red. Each well had a final volume 100 μL. Amounts of mitochondria, signal peptides (yCoxIV or SynB2), Mitotracker Red, and FCCP were first calculated and used to determine the

volume of energized import buffer that would be added. When called for in the condition, concentrations of reagents were 10 μg/100 μL of mitochondria, 10 μg/100μL yCoxIV, 1.5 μM FCCP, and finally, the volume in μL energized import buffer needed for a final volume of 100 μL per well. Assembly of reactions took place in the following order:

Control: Import Buffer – Mitochondria

yCoxIV: Import Buffer – yCoxIV – Mitochondria

FCCP: Import Buffer – Mitochondria – FCCP – yCoxIV

Each reaction mixture was gently stirred and allowed to incubate at room temperature for 30 minutes. During the incubation period, the Mitotracker Red was prepared. Mitotracker Red was added to make a final concentration of 500 nM. Reactions with Mitotracker Red were spread in the 96-well plate and incubated in the dark at room temperature for 5 minutes. Following incubation, the fluorescence was measured using the spectrophotometric plate reader at an excitation wavelength of 581 nm, and emission wavelength of 644 nm and a cutoff of 610 nm.

Following measurements, yeast were imaged using a 10x objective on the Nikon TE2000 Eclipse Inverted Fluorescence Microscope. Fluorescence intensity was measured across the imaged field after background removal using NIS Elements v.4.3.

4. Results and Discussion

Previous studies suggested that import of proteins into the mitochondrial matrix relies on the membrane potential across the inner membrane. Given the impermeable nature of this membrane to ions, this study focused on the effects of protein import on mitochondrial inner membrane potential. We examined these effects by knocking down the protein import channel Tim23, which was achieved by growing yeast in media lacking galactose (-Gal). We then performed

protein import reactions on isolated mitochondria of yeast grown in presence or absence of galactose. The effects of Tim23 knock down on mitochondrial membrane potential were observed by spectrofluorimetry and live fluorescence microscopy.

Growth of Tim23-deficient yeast was evaluated in agar plates and liquid cultures. The results confirmed the deleterious effect of Tim23 removal [20] on yeast grown in the presence of lactate. Yeast cultures are able to thrive in the presence of fermentable carbon sources, i.e., without using mitochondrial respiration. Using lactate as a non-fermentable carbon source ensured our observation of maximum effects of Tim23 deficiency. Figure 2 shows that Tim23 deficiency significantly impairs growth in both agar plates and liquid cultures. As shown in Figure 2B, optic densities reached 6.0 after approximately 15 hours in +Gal cultures, but in –Gal, the OD remained below 1.0.

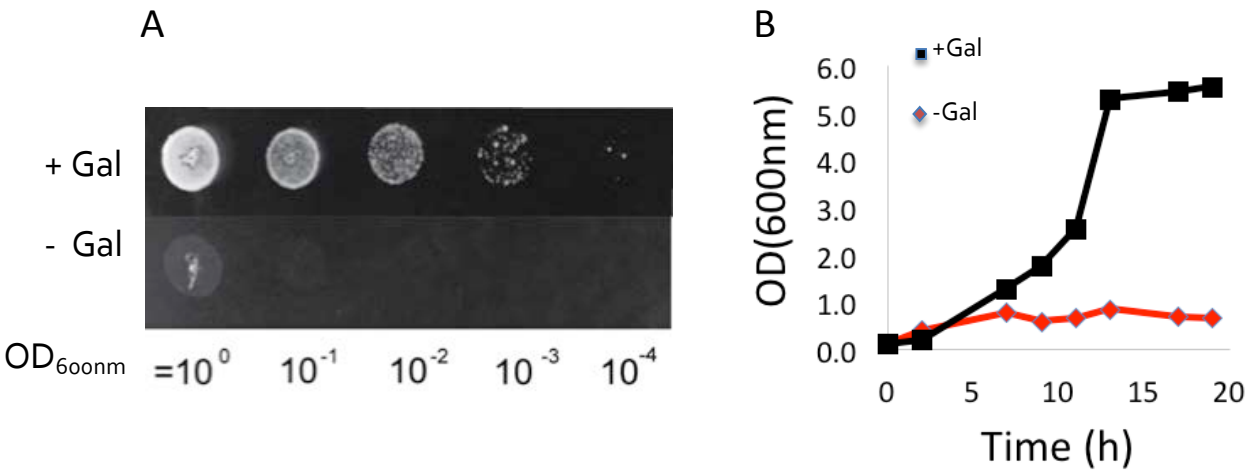

Figure 2: Effect of Tim23 knockdown of yeast growth. A) Photographs of Tim23 Gal10 grown in the presence (top) and absence (bottom) of galactose. The plates were inoculated with 10 μL of 1:10 serial dilutions taken from cultures grown to an OD of 1. B) Growth curves plotted from average optic densities (n=3) every two hours.

After confirming the growth defects, we measured the steady state membrane potential of intact mitochondria in cells. Cultures were diluted to an OD of 0.5 and incubated with 5 μM TMRM a membrane permeable, positively charged fluorescent marker that, driven by membrane potential, accumulates into mitochondria. Fluorescence microscopy images (Figure 3) show clear localization of TMRM in wild type mitochondria, evidencing a defined mitochondrial morphology with both elongated and circular structures. Localization of TMRM was not definitive in Tim23 knockdown yeast, indicating that the depletion of the pore in the TIM23 complex also depletes membrane potential. No previous studies describe the steady state membrane potential of intact yeast compared to Tim23 depletion. It is possible that in the absence of the Tim23 pore, the integrity of the inner membrane is compromised, resulting in a leak of protons into the matrix. Alternately, studies have shown that the TIM23 complex can associate with both Complexes I and III of the respiratory chain [21, 22]. The breakdown of this association could affect the integrity of the proton pumping abilities of these complexes. Even more compelling, however, is a study showing that cytochrome c oxidase, a subunit of Complex III is imported through the TIM23 complex [23]. Eliminating the pathway of import for cytochrome c oxidase would likely result in collapse of ETC function and membrane potential. Future studies will examine the levels of cytochrome c oxidase and other ETC components by western blot.

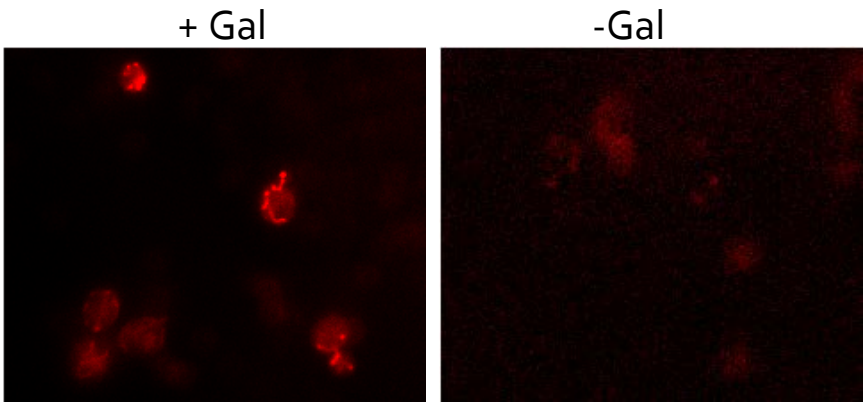

Figure 3: Mitochondrial membrane potential in wild type and Tim23 deficient yeast. Representative fluorescence microscopy images are shown of yeast grown in liquid + Gal (left) and – Gal (right) SDLac medium and incubated with 5 μM TMRM. Frames were acquired with 40 X magnification and 500 ms exposure.

In order to gain mechanistic insight into the observed decrease in steady state membrane potential we evaluated this physiological indicator during protein import. Mitochondria were isolated from both and incubated with import peptides in the presence and absence of ATP and NADH. Membrane potential was estimated by labeling with Mitotracker Red, a fluorescent marker that accumulates in mitochondria with intact membrane potential. Figure 4A shows that treatment of mitochondria with yCoxIV signal peptide induced a slight decrease in Mitotracker fluorescence in both + Gal (448.36 ± 17.21 to 418.21 ± 2.44, n=3, p=0.0398) and -Gal (443.26 ± 11.13 to 402.9 ± 7.86, n=3, p=0.007). In order to ensure the mitochondria were functionally intact, we also measured Mitotracker fluorescence in the presence of the depolarizing agent FCCP. The figure shows that addition of FFCP reduced fluorescence to 128 ± 7 in + Gal and 154 ± 5 in -Gal ($p<0.0001$).

Interestingly, we observed dissimilar results when we imaged these samples by fluorescence microscopy. Figure 4B provides a visual comparison of Mitotracker fluorescence localized in mitochondria. In wild type (+Gal), fluorescence intensity is increased in the presence of

yCoxIV, while addition of FCCP had the opposite effect. In Tim23 deficient (-Gal), fluorescence intensity differences are difficult to discern between control and yCoxIV conditions, but are again depleted after FCCP treatment. Figure 4C provides a quantitative comparison of the microscopy results by obtaining intensity values in mitochondria across the visual field and following background intensity deletion. Initially, steady state fluorescence intensity was higher in Tim23 knockdown compared to wild type mitochondria (268.9 ± 91.56 to 185.4 ± 82.96 $n>15$, $p<0.005$). Addition of yCoxIV to wild type mitochondria caused a marked increase in membrane potential (427.6 ± 88.25, $p<0.005$). Interestingly, this effect was not observed when yCoxIV was added to mitochondria deficient in Tim23 (289.2 ± 78.93, $p=0.45$). These results suggest that the membrane potential differences elicited by import peptide were dependent on Tim23.

Previous studies demonstrated that yCoxIV is imported into mitochondria under the same conditions used here [19]. Therefore, we provide novel evidence that protein import affects mitochondrial membrane potential. Unlike previous studies which focused on the metabolic requirements of protein import, we investigated the consequences of protein import on mitochondrial function. It was however intriguing that the observed effects were of hyperpolarization rather than slight depolarization as suggested in Figure 4A. This apparent discrepancy requires further investigation. However, it is possible that the levels of fluorescence in control and yCoxIV conditions (Figure 4A) were at a saturation point. Titrating the concentrations of Mitotracker Red in future studies will allow us to determine if this was the case.

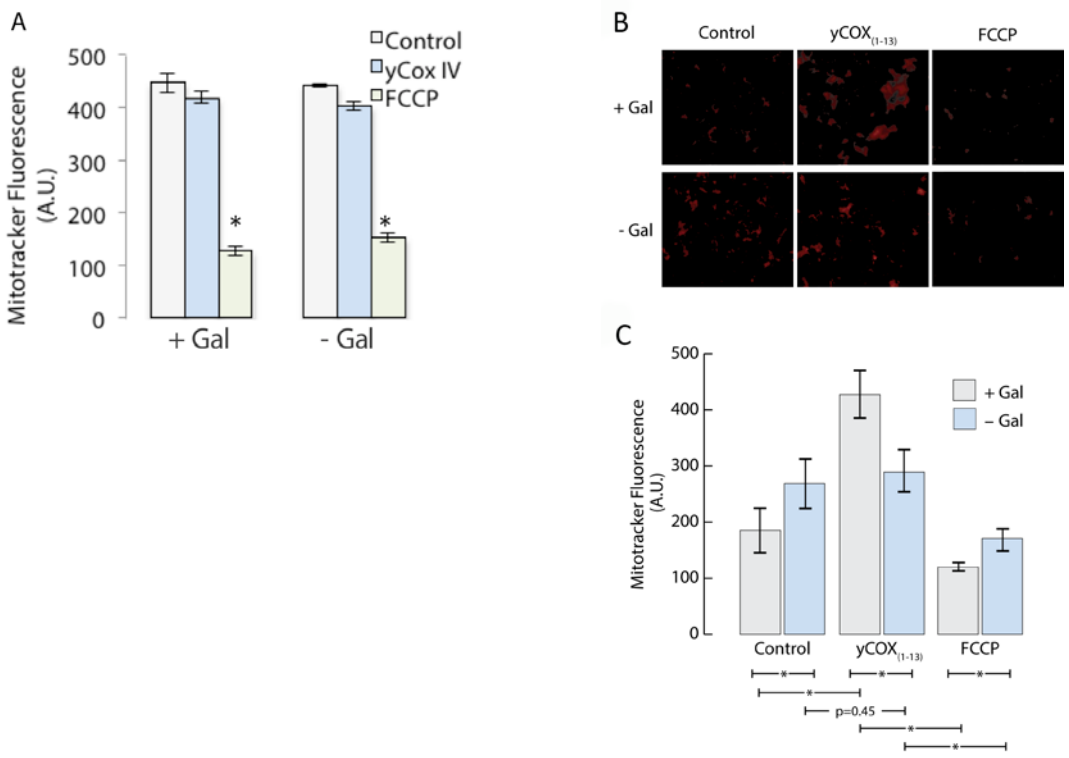

Figure 4: Effect of protein import on membrane potential. A. Bar histograms of average Mitotracker Red fluorescence (± SD, n=3). Protein import reactions were carried as described in the methods section. Isolated mitochondria were treated with vehicle (water) or 5 μg/μL yCoxIV$_{(1\text{-}13)}$. As a control, mitochondria were depolarized with 1.5 μM FCCP. The asterisk represents p<0.0005. B. Representative fluorescence microscopy images are shown of isolated mitochondria after import reactions as above. C. Bar histograms of average Mitotracker Red fluorescence measured in arbitrary units (± SD, n > 15). P values were calculated between conditions indicated by the brackets under the graph. For example, the p value between control and yCoxIV-treated -Gal was 0.45. The Asterisk indicates p<0.005.

5. Concluding Remarks

In summary, our results demonstrate that removal of Tim23 decreases the steady state membrane potential of intact mitochondria, which is also affected by protein import. Interestingly, the fluorescence microscopy data suggest that treatment with import peptides hyperpolarizes mitochondria, and that this effect is dependent on Tim23. Future studies will address the discrepancies between spectrofluorimetric and fluorescence microscopy results, which would either confirm or challenge the microscopy results. Additionally, we will examine the effects of Tim23 knockdown on mitochondrial respiration and emission of reactive oxygen species. Finally, determining levels of ETC components such as cytochrome c oxidase in Tim23 deficient mitochondria may help explain the observed membrane potential defects.

6. Bibliographic References

1. Zimorski, V., et al., *Endosymbiotic theory for organelle origins.* Curr Opin Microbiol, 2014. **22**: p. 38-48.
2. Calvo, S.E., K.R. Clauser, and V.K. Mootha, *MitoCarta2.0: an updated inventory of mammalian mitochondrial proteins.* Nucleic Acids Res, 2016. **44**(D1): p. D1251-7.
3. Neupert, W. and M. Brunner, *The protein import motor of mitochondria.* Nat Rev Mol Cell Biol, 2002. **3**(8): p. 555-65.
4. Gray, M.W., et al., *Genome structure and gene content in protist mitochondrial DNAs.* Nucleic Acids Res, 1998. **26**(4): p. 865-78.
5. Kuhlbrandt, W., *Structure and function of mitochondrial membrane protein complexes.* BMC Biol, 2015. **13**: p. 89.
6. Nakamoto, R.K., J.A. Baylis Scanlon, and M.K. Al-Shawi, *The rotary mechanism of the ATP synthase.* Arch Biochem Biophys, 2008. **476**(1): p. 43-50.
7. Alcazar-Fabra, M., P. Navas, and G. Brea-Calvo, *Coenzyme Q biosynthesis and its role in the respiratory chain structure.* Biochim Biophys Acta, 2016. **1857**(8): p. 1073-8.
8. Brandt, U., et al., *The mitochondrial targeting presequence of the Rieske iron-sulfur protein is processed in a single step after insertion into the cytochrome bc1 complex in mammals and retained as a subunit in the complex.* J Biol Chem, 1993. **268**(12): p. 8387-90.
9. Campo, M.L., P.M. Peixoto, and S. Martinez-Caballero, *Revisiting trends on mitochondrial mega-channels for the import of proteins and nucleic acids.* J Bioenerg Biomembr, 2016.
10. Schmidt, O., N. Pfanner, and C. Meisinger, *Mitochondrial protein import: from proteomics to functional mechanisms.* Nat Rev Mol Cell Biol, 2010. **11**(9): p. 655-67.
11. Vincow, E.S., et al., *The PINK1-Parkin pathway promotes both mitophagy and selective respiratory chain turnover in vivo.* Proc Natl Acad Sci U S A, 2013. **110**(16): p. 6400-5.

12. Koppen, M. and T. Langer, *Protein degradation within mitochondria: versatile activities of AAA proteases and other peptidases.* Crit Rev Biochem Mol Biol, 2007. **42**(3): p. 221-42.
13. Aung, M., et al., *Protein Import Channels in the Crossroads of Mitochondrial Function*, in *Molecular Basis for Mitochondrial Signaling*. In Press.
14. Botman, D., W. Tigchelaar, and C.J. Van Noorden, *Determination of glutamate dehydrogenase activity and its kinetics in mouse tissues using metabolic mapping (quantitative enzyme histochemistry).* J Histochem Cytochem, 2014. **62**(11): p. 802-12.
15. Kalef-Ezra, E., et al., *Import of a major mitochondrial enzyme depends on synergy between two distinct helices of its presequence.* Biochem J, 2016. **473**(18): p. 2813-29.
16. Asai, T., et al., *Reinvestigation of the requirement of cytosolic ATP for mitochondrial protein import.* J Biol Chem, 2004. **279**(19): p. 19464-70.
17. Martinez-Caballero, S., et al., *Tim17p regulates the twin pore structure and voltage gating of the mitochondrial protein import complex TIM23.* J Biol Chem, 2007. **282**(6): p. 3584-93.
18. Symersky, J., et al., *Structure of the c(10) ring of the yeast mitochondrial ATP synthase in the open conformation.* Nat Struct Mol Biol, 2012. **19**(5): p. 485-91, S1.
19. Peixoto, P.M., et al., *Awaking TIM22, a dynamic ligand-gated channel for protein insertion in the mitochondrial inner membrane.* J Biol Chem, 2007. **282**(26): p. 18694-701.
20. Lohret, T.A., R.E. Jensen, and K.W. Kinnally, *Tim23, a protein import component of the mitochondrial inner membrane, is required for normal activity of the multiple conductance channel, MCC.* J Cell Biol, 1997. **137**(2): p. 377-86.
21. Wiedemann, N., et al., *Sorting switch of mitochondrial presequence translocase involves coupling of motor module to respiratory chain.* J Cell Biol, 2007. **179**(6): p. 1115-22.
22. Kulawiak, B., et al., *The mitochondrial protein import machinery has multiple connections to the respiratory chain.* Biochim Biophys Acta, 2013. **1827**(5): p. 612-26.
23. Vazquez-Acevedo, M., D. Rubalcava-Gracia, and D. Gonzalez-Halphen, *In vitro import and assembly of the nucleus-encoded mitochondrial subunit III of cytochrome c oxidase (Cox3).* Mitochondrion, 2014. **19 Pt B**: p. 314-22.